GOSPODARKA SUROWCAMI MINERALNYMI – MINERAL RESOURCES MANAGEMENT

2019 Volume 35 Issue 2 Pages 5–30

DOI: 10.24425/gsm.2019.128522

LUCYNA NATKANIEC-NOWAK[1], ADAM PIESTRZYŃSKI[2], MARIAN WAGNER[3], WIESŁAW HEFLIK[4], BEATA NAGLIK[5], JAN PALUCH[6], KRZYSZTOF PAŁASZ[7], STANISLAVA MILOVSKÁ[8], PAWEŁ STACH[9]

# "Górka Lubartowska-Niedźwiada" deposit (E Poland) as a potential source of glauconite raw material

## Introduction

The largest and at the same time the first documented deposit of Eocene quartz-glauconite sands in Poland is located in the Lublin Province, in Niedźwiada and Brzeźnica Leśna

✉ Corresponding Author: Lucyna Natkaniec-Nowak; e-mail: natkan@agh.edu.pl
[1] AGH University of Science and Technology, Krakow, Poland; ORCID iD: 0000-0002-0113-0910; e-mail: natkan@agh.edu.pl
[2] AGH University of Science and Technology, Krakow, Poland; ORCID iD: 0000-0001-6649-6772; e-mail: piestrz@geol.agh.edu.pl
[3] AGH University of Science and Technology, Krakow, Poland; ORCID iD: 0000-0002-7694-6527; e-mail: wagner@geol.agh.edu.pl
[4] AGH University of Science and Technology, Krakow, Poland.
[5] Beskidzka Str., Międzybrodzie Żywieckie, Poland; ORCID iD: 0000-0002-4452-3378; e-mail: beata.naglik@op.pl
[6] STELLARIUM mining company, Niedźwiada, Poland; ORCID iD: 0000-0001-7675-0623; e-mail: jan.paluch@stellarium.co
[7] AGH University of Science and Technology, Krakow, Poland; e-mail: 6saper6@gmail.com
[8] Ústav vied o Zemi Slovenskej Akadémie Vied, Banská Bystrica, Slovakia; ORCID iD: 0000-0002-0260-5033; e-mail: milovska@savbb.sk
[9] AGH University of Science and Technology, Krakow, Poland; ORCID iD: 0000-0002-5886-9468; e-mail: pstach@agh.edu.pl

Kolonia (Niedźwiada Commune, Lubartów County, Lublin Province). STELLARIUM with its headquarters in Niedźwiada-Kolonia, which took over this area, has been interested in this deposit for the past few years and after obtaining all the necessary permits started exploitation using opencast method. The area was previously investigated with 32 boreholes, as well as by way of a geological, geophysical and hydrogeological survey (2015–2017). STELLARIUM developed the geological documentation based on the geological survey (2017). In addition to the main raw material, which is the quaternary feldspar-quartz sand due to its largest thickness, the accompanying components in the "Górka Lubartowska-Niedźwiada" deposit are glauconite and amber. In these sediments, only small, heavily crushed fragments of the fossil resin were found, with no jeweller's value. The most attention, however, is drawn by glauconite, primarily as a potential raw material for the production of mineral fertilizers (e.g. Krzowski 1995 and references therein; Bogdasarow et al. 2016 and references therein).

Since its discovery in the 1820s until the present day, i.e. for almost 200 years, glauconite has been raising the interest of a growing number of scientists. The first detailed structural studies of glauconite were made by C.M. Warshaw (1957) and J. Burst (1958), but previously it was a subject of research conducted among others by Kazimierz Smulikowski, an eminent Polish geologist, petrographer and mineralogist. In 1953, Smulikowski wrote a paper entitled "Considerations on the subject of glauconite", followed by many more papers in the years to come. These and the results of the studies of subsequent researchers (e.g. Hower 1961; Triplehorn 1966; Foster 1951, 1969; McRae 1972; Odin and Matter 1981; Odin and Fullagar 1988; Amorosi et al. 2007; Ospitali et al. 2008; Franus 2010; Yakhontova 2010; Smaill 2015) showed that the individual glauconite grains differ with regard to the degree of crystallinity and structural maturity as well as to the composition of the swelling layers, and thus have a varied chemical composition.

Glauconite is common chiefly in shallow marine sediments on the border of the shelf and the continental slope, i.e. at depths ranging between 50 and 500 m (Odin and Fullagar 1988; Amorosi et al. 2007). It forms from a clay suspension or silica-alumina coagulum brought in from the land under boundary redox conditions (Wilkin et al. 1996; Zatoń et al. 2008), at a relatively low tidal energy and water rippling, and slow sedimentation rate. The transformation process consists of several stages, according to the following scheme:

$$\text{illite} \rightarrow \text{folidoid} \rightarrow \text{aluminum glauconite} \rightarrow \text{typical glauconite}$$

At each stage, the product being formed exhibits different physico-chemical properties (Odin and Matter 1981). In the initial stage of the transformations (glauconitization), the resulting folidoid is light green in color and its crystallinity increases with its maturity. It becomes richer in potassium and iron, which over time achieve significant dominance over aluminum and the color eventually becomes dark green (Shively and Weyl 1951; Warshaw 1957; Yakhontova 2010). The exchange reactions lead to substitution in the tetrahedral layer of aluminum for silicon, and in the octahedral layer of iron and magnesium in place of

aluminum. To balance the charge, potassium cations are taken up from the solution, which are located in the interlayer spaces. The structure of the typical glauconite is dominated by trivalent iron, the content of which is much higher than the amount of aluminum cations ($Fe^{3+}/Al$ >3) and constitutes more than half of all cations in octahedral positions (e.g. Grim 1953; Foster 1969; Franus 2010).

Glauconite occurs in nature as several polytypes (1M, 2Md and 2M1), with the 1M polytype being the most widespread. It is a highly ordered glauconite, which contains less than 10% of swelling layers in its structure and is characterised by a high potassium content. The less frequent 2Md polytype has an unordered structure, the share of swelling layers is greater (10 to 20%), whereas the potassium content is lower. An exceptionally disordered structure is typical of the 2M1 polytype, which contains 20 to 60% of swelling layers and has the lowest potassium content.

G.S. Odin and A. Matter (1981), and A. Amorosi et al. (2007) distinguish several varieties of glauconite on the basis of its potassium content, i.e. with the $K_2O$ content <4 wt%. (in the initial phase of transformation), 4–6 wt% $K_2O$ (growing), 6–8 wt% $K_2O$ (mature) and > 8 wt% (highly mature). The immature glauconite contains abundant iron-rich smectites, while in the course of its maturation in its inter-layer spaces an increase in the amount of potassium cations is observed and then it evolves into a mineral with a structure resembling that of illite (Baldermann et al. 2012). It very frequently forms aggregates composed of fine grains and scales, around which regenerative rims with a distinctive radial structure are present.

Glauconite has very specific properties of ion exchange and sorption also in relation to metal cations of varied valence (Soni 1990; Kłapyta 2008; Franus 2010). This implies a wide range of its applications, mainly as a mineral fertilizer rich in: K, Fe, Mg and biomicronutrients, which are released into the soil and fertilize and open it, which in turn improves the physical and chemical properties of the soil (Soni 1990). It can also be used as a filtering agent and ion exchanger for softening drinking water. For centuries, it has been used for the production of natural mineral paints, ceramic pigments, as well as glass, hence its indirect application in sculpture and masonry work, etc. Glauconite also found application in such areas as: the brewing industry (filtering agent), sugar-making, textile industry (raw material), and even in medicine (a non-antibiotic antibacterial drug) (Valanchene et al. 2006). In geological sciences, it is utilised in the K-Ar isotope dating method (Tyler and Bailey 1961; Evernden et al. 1961; Kazakov 1964; Bodelle et al. 1969) and as a paleoenvironmental indicator (Burst 1958; Zatoń et al. 2008).

The aim of the study was to provide a mineralogical and petrological description of the quartz-glauconite sediments from the "Górka Lubartowska-Niedźwiada" deposit, which form the glauconite layer itself in the profile of this deposit and of the quartz-glauconite sandstone accompanying them, with a particular stress put on the morphological, granulometric and structural diversity of the glauconite itself, and also on the variability of its chemical composition affecting the assessment of its usefulness in various sectors of the economy. A specific geological curiosity is the vegetable detritus (xylite) present in the sand,

which has also been the subject of research. This is certainly a novelty when it comes to these sediments. In addition to macro- and microscopic observations under the stereoscopic microscope, polarizing transmitted and reflected light microscopes, and the scanning electron microscopy (SEM-EDS), X-ray diffraction analysis (XRD), Raman spectroscopy (RS) and X-ray fluorescence spectrometry (XRF) investigations were performed, and chemical analyses were made with an electron microprobe. On the basis of the abundant data from empirical research, a thorough petrogenetic analysis of the material was carried out, and in particular the possibility of utilising this glauconite sediment as a potential raw material, e.g. in the agricultural and chemical sectors as an environmentally friendly agent used to precipitate water from sewage sludge and to bind heavy metals was investigated for the first time.

## 1. Geological setting

The "Górka Lubartowska-Niedźwiada" deposit of the Eocene glauconite sediments is located in the Podlasie Lowland, which is a peripheral part of the Precambrian Platform. The lower-order unit is Łuków Horst, intersected by the following transverse faults (from the north): Łasice, Rzeczyca, Kolembroda, Huszcza, and Hanna fault, and separated in the west by a regional, NW-SE dislocation zone (Kock Fault Zone) (Łozińska-Stępień et al. 1986).

The lithological profile of the deposit is shown in Figure 1. The type and quality of the mineral have been documented on the basis of detailed macroscopic and laboratory tests. The quality parameters of the main mineral and the associated components are contained in the "Geological Documentation of the feldspar and quartz sands and accompanying minerals: glauconite and amber – Górka Lubartowska-Niedźwiada".

The "Górka Lubartowska-Niedźwiada" deposit profile begins with Quaternary clastic sediments of the aleuritic-psammitic fraction that contain gravel and pebbles of mainly igneous rocks and include clay/silt lenses (with a thickness of up to 10 m), covered with a humus layer (ca. 0.5 m). These are upper fluvioglacial, outwash plain sediments (Łozińska-Stępień et al. 1986), in places deposited on the boulder clay of the maximum stadial. They are related to the recession of the ice sheet of the maximum stadial of the Central Poland glaciation. In the floor of these sediments, the share of clay minerals increases and rock pebbles as well as quite abundant plant remains (xylite) are present.

The Q series of sands is covered with a complex of Paleogene sediments (lower Eocene), which is the glauconite layer itself (ca. 7 m in thickness). These are predominantly fine- and medium-grained sands of a dark grey-greenish-blue color, containing abundant clay, in which marine fauna is present and crumbs of amber can be found. In the floor of these sediments, fine lamellas and lenses of the clay-laden, diagenetically altered glauconite silt with pebbles and concretions of phosphates appear (a transition zone, ca. 0.2 m in thickness), and a nearly 1.5-meter-thick layer of fine- and medium-grained glauconite sand, and a very fine 0.05-meter-thick lamina of quartz-glauconite sandstone occurs below.

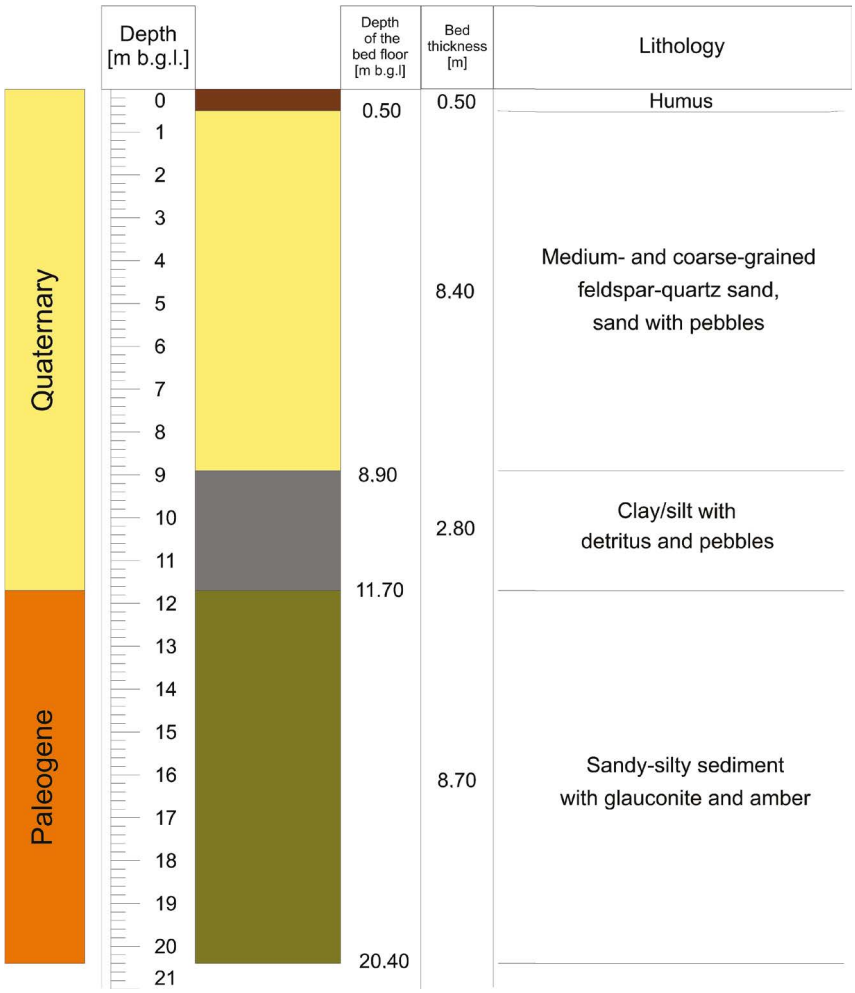


Fig. 1. Geological profile of the "Górka Lubartowska-Niedźwiada" deposit (scale 1:200; borehole no 02_23)

Rys. 1. Profil geologiczny złoża „Górka Lubartowska-Niedźwiada" w skali 1:200 (otwór nr 02_23)

Cretaceous sediments represented in the roof by marly silt and marl occurs in the lower part of the deposit profile, at a depth of nearly 22 meters, the color of which upon contact with the overlying Eocene is dark grey and then gradually changes into light grey (Łozińska-Stępień et al. 1986; Kuhn and Pizon 1987).

## 2. Materials and methods

The analytical material consisted of approximately 30 kg of Eocene glauconitic sediments collected from the entire interval, i.e. from a depth of ca. 12–20 m and included

10 small pieces of xylite from the lower part of the lower Quaternary sediments (ca. 11 m deep). This material was made available for laboratory tests by STELLARIUM Sp. z o.o. based in Niedźwiada-Kolonia.

Preliminary observations of the quartz-glauconite sand and quartz-glauconite sandstone were carried out with the use of the SNZ-168 stereoscopic microscope (magnification: ×7.5, ×10, ×20, ×30, ×40 and ×50), coupled with a digital camera (the Panasis software was used for the photographic documentation).

Microscopic examinations of the exposed polished sections were performed with the BA310POL polarization microscope for transmitted light samples coupled with a digital camera (the Panasis software was used for the photographic documentation).

Petrographic investigations of the polished sections (a transverse section) of xylite were performed with the PZO and Axioplan (Zeiss-Opton) polarized light microscopes for the transmitted and reflected light samples, respectively. Measurements of the random reflectance ($R^o_r$) of euulminite B were made with the Axioplan M-400 photometer in standard conditions (ISO 7404-5).

The investigations of the ore minerals were carried out with the use of the NICON ECLIPSE polarized light microscope equipped with a DP12 camera.

The SEM-EDS investigations were performed with the American FEI Quanta 200 FEG scanning electron microscope equipped with an energy-dispersive X-ray spectrometer (EDS). The system was operated at 20 kV accelerating voltage in a high-vacuum mode.

Identification of mineral phases contained in the samples was carried out with the X-ray powder diffraction method (XRD) using a RIGAKU SmartLab X-ray diffractometer. Measurement parameters: $Cu_{K\alpha}$ radiation, graphite reflective monochromator, lamp voltage 45 kV, current 200 mA, step 0.05°2Θ, pulse counting time 1 sec/step. In order to identify minerals with swelling layers, also X-ray graphs after prior saturation of samples with ethylene glycol were recorded.

Raman spectroscopy (RS) investigations were performed with the Thermo Scientific DXR spectrometer (Thermo Fisher, Waltham, MA, USA), cooperating with the Olympus BX-40 optical microscope (magnification: 100×, 50×, 10×). The source of the excited light was the Spectra-Physics argon laser with a wavelength of 514.5 nm and a beam power of approx. 24 mW (the parameters were chosen according to the optical nature of the sample). The Raman spectra were collected in a backscatter mode in the primary infrared range 100–4000 $cm^{-1}$.

The investigations of the chemical composition of glauconite (EPMA) were carried out at the AGH Laboratory of Critical Elements using the JEOL Super Probe JXA-8230 electron microprobe, cooperating with the WDS detector. Measurement parameters: voltage 15 kV, beam current 5 nA, maximum counting time 10 s, background time 5 s, measuring lines: Ca Kα, Mg Kα, K Kα, Fe Kα, S Kα, Si Kα and Al Kα.

The aforementioned analyses were carried out at the Laboratory of Phase, Structural and Textural Research of the Faculty of Geology, Geophysics and Environmental Protection of the AGH University of Science and Technology in Krakow, Poland.

The XRF analyses were performed with the Bruker M4 TORNADO spectrometer at the SAV Optical Laboratory in Banská Bystrica (Slovakia). The measurements were carried out in a vacuum and with the following parameters: detection field diameter 25 μm, interaction depth 10–1000 μm, excitation of potential on a rhodium lamp 600 μA at 50 kV.

## 3. Results

### 3.1. Quartz-glauconite sand

The sand under investigation was collected during drilling work from the glauconite horizon itself. This is a clastic sediment of the aleuritic-psammitic fraction, containing a distinctive amount of clayey substance, with a characteristic grey-blue coloration. In addition to glauconite, which is the main coloring agent, there is also a second main component, i.e. quartz, whose grains are easily felt to the touch. In addition to the phases mentioned, there are also aggregate forms showing various degree of sorting (size) and roundness, which creates an impression of "clumping", while the clay-laden nature of this material is probably the effect of the presence of a significant content of clay minerals in it. The sand also contains lumps of amber of various (chiefly small) sizes and quite numerous fossils (Fig. 2A, B).

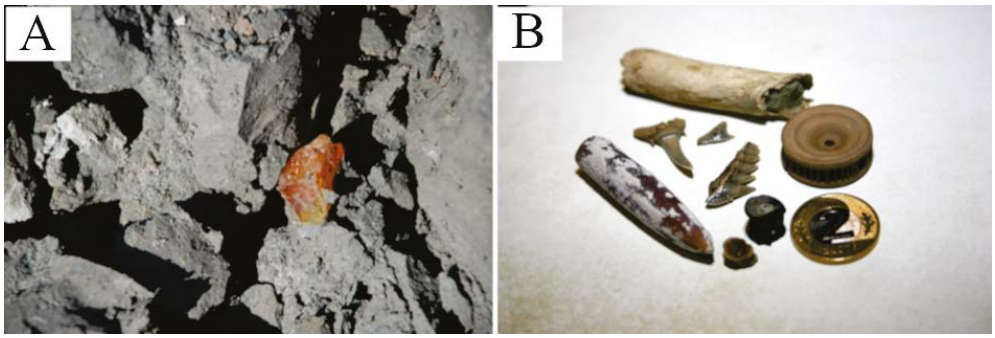


Fig. 2. Quartz-glauconite sand with lumps of resin (A) and fauna (B)

Rys. 2. Piasek kwarcowo-glaukonitowy z bryłkami żywicy (A) i fauną (B)

Under the transmitted-light optical microscope, the averaged rock material consists of quartz grains (ca. 45 vol%) and glauconite (ca. 30 vol%), clay aggregates (ca. 20 vol%), individual feldspar tables, mica strands, and rosette-like aggregations of black elongated crystals (gypsum?), as well as opaque minerals. This material is characterized by a poor degree of sorting and a medium degree of roundness (Fig. 3). The mineral composition is dominated

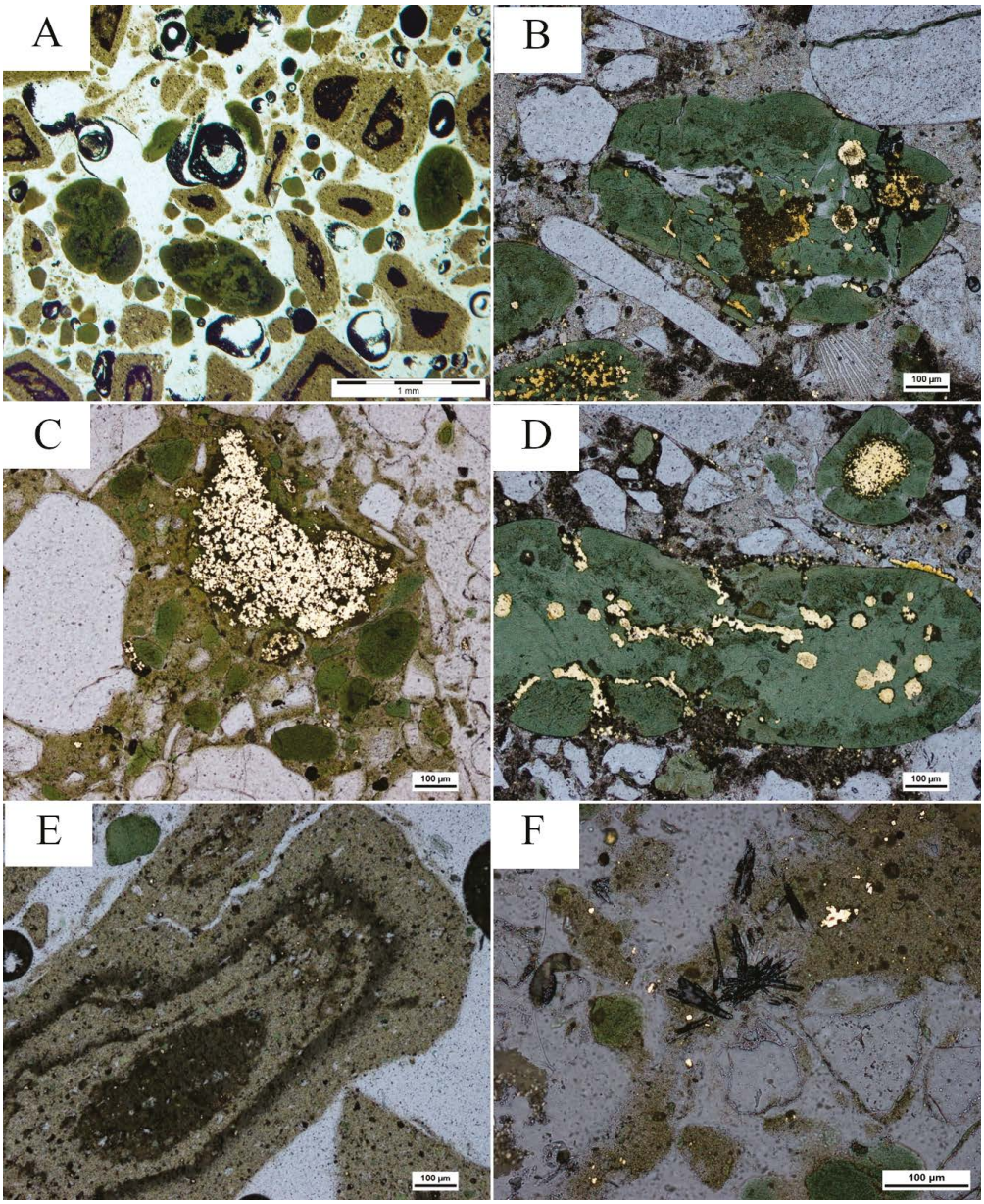


Fig. 3. Photomicrographs of quartz-glauconite sand from the "Górka Lubartowska-Niedźwiada" deposit (NX/1N). A – poor degree of sorting and a medium degree of roundness of the analytical material; B, C, D – euhedral and/or framboidal forms of pyrite aggregations within glauconite grains; E – clay aggregates; F – rosette gypsum crystals

Rys. 3. Obrazy mikroskopowe piasku kwarcowo-glaukonitowego ze złoża „Górka Lubartowska-Niedźwiada" (NX/1N). A – widoczny słaby stopień wysortowania i średni stopień obtoczenia materiału analitycznego; B, C, D – euhedralne i/lub framboidalne formy skupień pirytu w obrębie ziaren glaukonitu; E – agregaty ilaste; F – rozetowe kryształy gipsu

by quartz grains with an average size of approx. 0.5 mm (up to 2 mm). All the grains extinguish the light in a uniform manner. They are usually angular, especially the smaller ones (Fig. 3A, B). The rounded contours are typical of individuals located in the rims of small mosaic quartz grains. Wedge forms characteristic of pyroclastic sediments also occur. Glauconite grains (light green) have an average size of 0.15 mm, with the small individuals (about 0.10 mm) being in the vast majority. They are characterized by fairly good roundness. Some grains, especially the larger ones, have regenerative rims of a much lighter color (slightly yellowish). Single grains contain numerous inclusions of opaque minerals (Fig. 3C, D). They have different sizes and variable morphology, most of them have round forms, very similar to framboids (e.g. of pyrite). Rock clasts are usually large (> 1 mm), chiefly elongated and well-rounded aggregates (Fig. 3E), in which in addition to clay minerals, angular quartz grains as well as glauconite most often also of an angular shape occur. Clay minerals (?), that form a kind of matrix in them, take on forms of very fine scales.

The share of opaque minerals in the sand under investigation is significant. They form both the dispersed, isolated grains (approx. 0.025 mm in size), inclusions in glauconite individuals (sporadically), but most of all they are present in clay aggregates. These are most likely iron compounds. Single, well-rounded zirconium grains also occur occasionally. Their total content is approx. 3 vol%. Their mineralogical nature was possible to determine by way of the microscopic examination in reflected light. The presence of sulphide iron compounds, mainly pyrite and in smaller quantities of marcasite (in the amount of 0.1 to 3.0 vol%), is most frequently observed in the glauconite concretions or in the form of a pigment dispersed in the rock mass. Pyrite is present as small aggregations of more or less regular grains or framboid-like forms, which are sometimes considered as mineralized bacterial cells (Schieber 2002; Gong et al. 2008). These sulphides are formed at the stage of diagenesis of clastic sediments. The source of iron can be glauconite, and sulphur may come from an organic matter or a sulphate of a gypsum nature. The latter can be seen in Fig. 3F in the form of large rosette-like individuals. The sulphides are accompanied by single grains of titanium oxide (anatase).

SEM images (Fig. 4) show significant morphological diversity of the glauconite grains in the sand under investigation. Some grains are markedly rounded (Fig. 4A), whereas others are angular (Fig. 4B). They do not show distinct variability of the chemical composition, which is confirmed by EDS analyses. The surface of most of the grains is smooth, without visible traces of etching. Within some of the glauconite grains, both rounded (framboidal) and euhedral pyrite crystals are present (Fig. 4C–F). In places, these crystals are so abundant that they may occupy up to 80% of their volume. Some of the glauconite individuals are heavily fractured, and euhedral individuals of pyrite occur in the fissures. In the SEM images, interesting mineral forms were also encountered, which represent pseudomorphs after organic forms (Fig. 5A, B), substituted with calcium phosphate (apatite). The residual content of the primary organic matter was recorded in the EDS spectra.

The XRD data implies that the glauconite in the sand represents the 1M polytype (Moore and Reynolds 1997). This variety is characterized by the presence of sharp and symmetrical

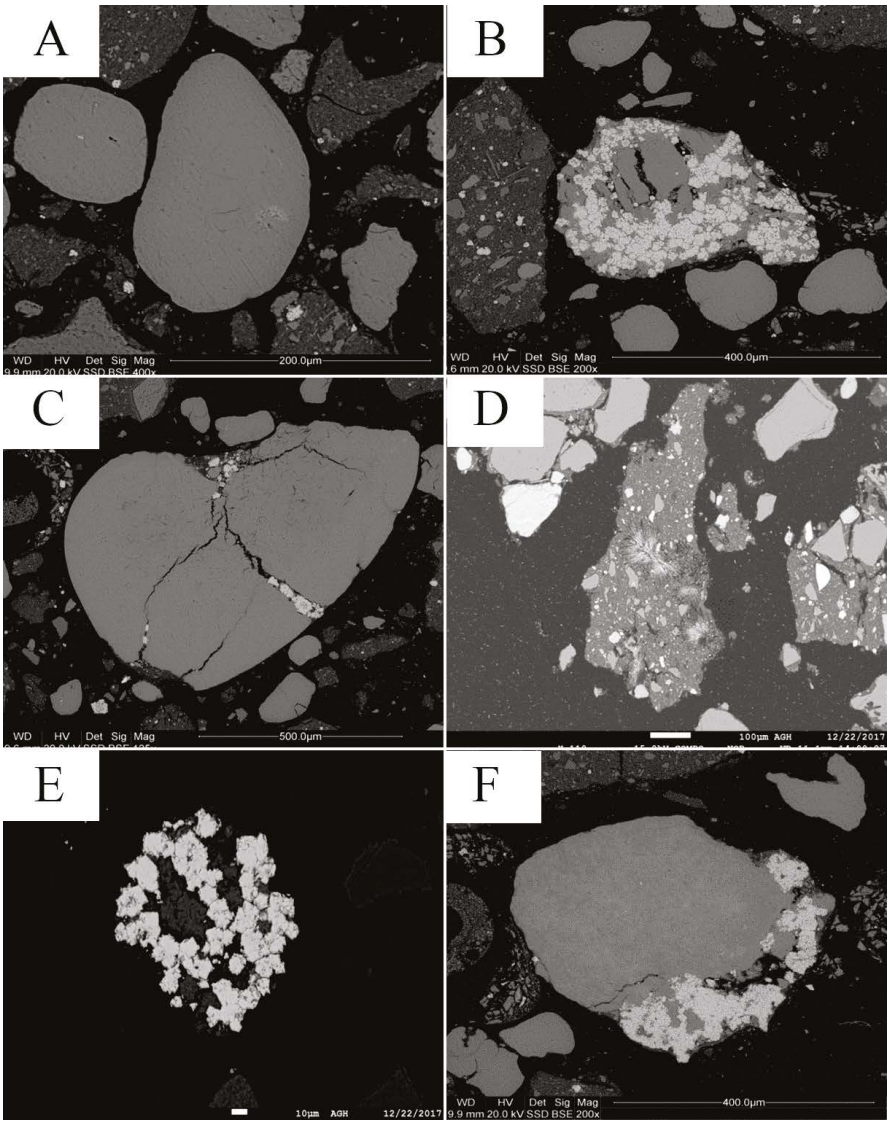


Fig. 4. SEM images of quartz-glauconite sand from the "Górka Lubartowska-Niedźwiada" deposit. A – glauconite grains of different size and roundness; B – regenerative rims around the glauconite grains and aggregates of various sizes, in which rosette-like concentrations of gypsum crystals are present; C, D – various forms of pyrite grains inside and on the edges of the glauconite grains; in addition to that, fine fragments of bioclasts (D) are visible; E – large grain of glauconite, in which fracture fissures are filled with secondary minerals, including Fe compounds; F – euhedral grains of pyrite in the glauconitic matrix

Rys. 4. Obrazy SEM piasków kwarcowo-glaukonitowych ze złoża „Górka Lubartowska-Niedźwiada". A – widoczne różnej wielkości i stopnia obtoczenia ziarna glaukonitu; B – widoczne obwódki regeneracyjne wokół ziaren glaukonitu oraz różnej wielkości agregaty, w których obecne są rozetowe skupienia kryształów gipsu; C, D – różne formy skupień ziaren pirytu wewnątrz i na obrzeżach ziaren glaukonitu; widoczne ponadto drobne fragmenty bioklastów (D); E – duże ziarno glaukonitu, w którym szczeliny spękań wypełniają wtórne minerały, w tym związki Fe; F – euhedralne ziarna pirytu w matrycy glaukonitowej

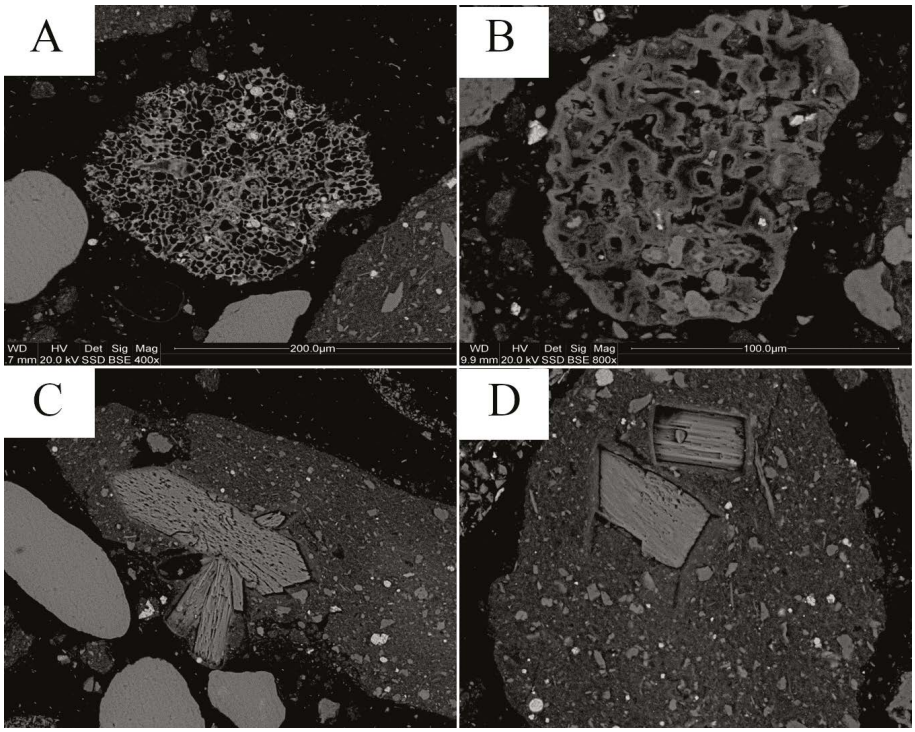


Fig. 5. SEM images of quartz-glauconite sand from the "Górka Lubartowska-Niedźwiada" deposit. A, B – pseudomorphs after organic forms composed of calcium phosphate (apatite?), C, D – gypsum crystals embedded in quartz-clay aggregates

Rys. 5. Obrazy SEM piasków kwarcowo-glaukonitowych ze złoża „Górka Lubartowska-Niedźwiada". A, B – pseudomorfozy po formach organicznych zbudowane z fosforanu wapnia (apatyt?), C, D – kryształy gipsu tkwiące w agregatach kwarcowo-ilastych

reflections $d_{hkl}$ = 4.35, 4.12, 3.65, 3.33, 3.09 and 2.68 Å. The fact that it is also accompanied by other clay minerals from the hydromicas group, e.g. illite and/or kaolinite cannot be ruled out. In addition to reflections from the main minerals (quartz, glauconite), sparse and low intensity reflections being indicative of the presence of feldspars, pyrite, oxide (and/or hydroxide) iron compounds, as well as gypsum are also present.

Eight glauconite grains were analysed with the electron microprobe. The results of the analyses are shown in Table 1. The variability of the chemical composition can be observed both between the individual glauconite grains (e.g. 1, 3 and 5) and within the grains (e.g. 4, 8). Comparing these values with data available in the literature, a distinctly lower content of aluminum ($Al_2O_3$), and a higher content of magnesium (MgO) and calcium (CaO) in the analysed grains can be observed. In addition to that, the appearance of "exotic" ions, such as $TiO_2$ and $Cr_2O_3$ was determined. After conversion of the data, the average chemical composition of glauconite from the examined sands (in wt%) can be obtained: $SiO_2$ = 52.698; $Al_2O_3$ = 5.441; $Fe_{tot}$ = 20.798; MgO = 4.623; $K_2O$ = 8.259;

$Na_2O$ = 0.08; CaO = 0.291; MnO = 0.024; BaO = 0.027; $TiO_2$ = 0.0242; $Cr_2O_3$ = 0.032; $H_2O$ = 7.651.

Table 1. Results of the WDS analyses for glauconite grains (in wt%)

Tabela 1. Wyniki oznaczeń WDS składu chemicznego ziaren glaukonitu (w % wag.)

| Grain | $SiO_2$ | $Al_2O_3$ | $Fe_{tot}$ | MgO | $K_2O$ | $Na_2O$ | CaO |
|---|---|---|---|---|---|---|---|
| 1 | 52.864 | 4.107 | 21.560 | 4.618 | 8.227 | 0.091 | 0.141 |
| | 53.626 | 4.326 | 21.389 | 4.965 | 8.326 | 0.116 | 0.235 |
| | 52.151 | 4.334 | 21.690 | 4.919 | 8.388 | 0.127 | 0.295 |
| | 52.359 | 6.292 | 21.265 | 3.607 | 8.201 | 0.097 | 0.371 |
| 2 | 51.058 | 5.165 | 20.306 | 4.775 | 8.550 | 0.049 | 0.187 |
| | 51.283 | 5.276 | 21.425 | 4.526 | 8.437 | 0.132 | 0.287 |
| 3 | 53.247 | 6.678 | 19.407 | 4.756 | 8.246 | 0.152 | 0.436 |
| 4 | 52.152 | 4.442 | 22.408 | 4.673 | 8.071 | 0.069 | 0.259 |
| | 52.699 | 4.743 | 20.879 | 4.590 | 8.442 | 0.087 | 0.266 |
| | 53.176 | 4.378 | 22.532 | 4.595 | 8.104 | 0.118 | 0.233 |
| 5 | 52.775 | 6.815 | 20.247 | 3.964 | 8.051 | 0.118 | 0.313 |
| | 52.258 | 6.233 | 21.017 | 4.331 | 8.096 | 0.069 | 0.323 |
| 6 | 52.223 | 5.444 | 21.409 | 4.417 | 8.371 | 0.035 | 0.282 |
| | 52.354 | 5.320 | 22.218 | 4.357 | 8.356 | 0.031 | 0.288 |
| 7 | 52.911 | 5.121 | 20.310 | 4.997 | 8.425 | 0.054 | 0.266 |
| | 53.273 | 5.204 | 20.596 | 5.266 | 8.394 | 0.030 | 0.244 |
| | 53.162 | 5.983 | 19.762 | 5.066 | 8.323 | 0.039 | 0.321 |
| 8 | 54.474 | 6.633 | 18.552 | 4.699 | 7.978 | 0.061 | 0.378 |
| | 53.208 | 6.883 | 18.186 | 4.709 | 7.930 | 0.054 | 0.412 |

### 3.2. Quartz-glauconite sandstone

Macroscopically, it is a compact, grey-blue clastic rock of the aleuritic-psammitic fraction, very similar to the above-described quartz-glauconite sand. Its distinctive color is the result of the presence of glauconite. Very fine grains of quartz are visible, and above all numerous fossils, probably bivalves and gastropods, as well as (mostly small) lumps of amber.

Under the polarizing transmitted light microscope, the rock does not exhibit sedimentary microstructures but a random texture and an aleuritic-psammitic structure (Pałasz 2017). The framework of grains makes up for nearly 70 vol% (Fig. 6A). Grains are characterized by poor sorting and fairly good roundness; their size is in the range of 0.1–2.0 mm (ca. 0.5 mm on an average). The framework of grains is dominated by quartz (ca. 70 vol%) and glauconite grains (ca. 20 vol%). Opaque minerals are present in smaller quantities (ca. 10 vol%) along with individual tables of feldspars and mica strands. There are abundant fragments of marine fauna, chiefly of bivalves and gastropods (Fig. 6B). According to the classification of Pettijohn, Potter and Siever (1972), the studied rock can be termed quartz wacke.

Quartz grains reveal big granulometric and morphological diversity. A considerable number of the grains are oval-shaped, well rounded – especially the larger ones, only a few grains have the preserved angular nature typical of pyrogenic quartz. A part of the quartz individuals, extinguish the light uniformly (ca. 70 vol%) and some grains show wavy light extinction (ca. 15 vol%). Polycrystalline quartz (ca. 15 vol%) is also encountered.

Glauconite, like quartz, is characterized by good roundness. The average grain size is 0.15 mm (max. 0.5 mm). All the grains show the mostly light-green color. Recrystallization rims are observed in many of them. Inclusions of opaque minerals, mainly pyrite, as indicated by the grain shapes, are present in numerous grains. In addition to the individuals with a smooth surface (Fig. 6C), fissured grains with dark mineral filling (pyrite?) also occur (Fig. 6D).

The cement of the sandstone is of the basic type (30 vol%). Sometimes it is a matrix type cement (17 vol%) (Fig. 6E), and in other places it represents the silica cement when it forms rims around quartz and glauconite grains (13 vol%) (Fig. 6F).

The SEM images show well-rounded glauconite grains, locally isometric or elongated (Pałasz 2017). A large number of grains are strongly fissured, with visible traces of etching (Fig. 7A); individuals with a smooth surface are rare. Fissures in the glauconite grains are filled with pyrite crystals, both framboidal (Fig. 7B) and euhedral (Fig. 7C), with a vast majority of the latter. Pyrite crystals also form abundant inclusions in glauconite (Fig. 7C) or occur in the form of isolated grains dispersed in the rock. Some glauconite individuals have silica rims (Fig. 7D). There are also numerous glauconite grains that contain calcium phosphate (Fig. 7E), quartz (Fig. 7F) or chalcedony in their centres.

The glauconite EDS spectrum (Fig. 8) implies that it contains large amounts of potassium and iron, and slightly smaller quantities of magnesium and aluminum, which according to G.S. Odin and A. Matter (1981) and A. Amorosi et al. (2007) points to the mature and even highly mature glauconite. In turn, XRF research (Pałasz 2017) shows that most glauconite individuals have composite, non-homogeneous structure, which is manifested by the presence in one grain of different color zones in the shades of light and dark green (Fig. 9A). The point measurements made in both of these areas show the variability of its chemical composition. In the dark-green areas, the share of elements characteristic of the degree of maturity of the glauconite, i.e. Fe, K, Mg and Al, clearly increases, which is confirmed by

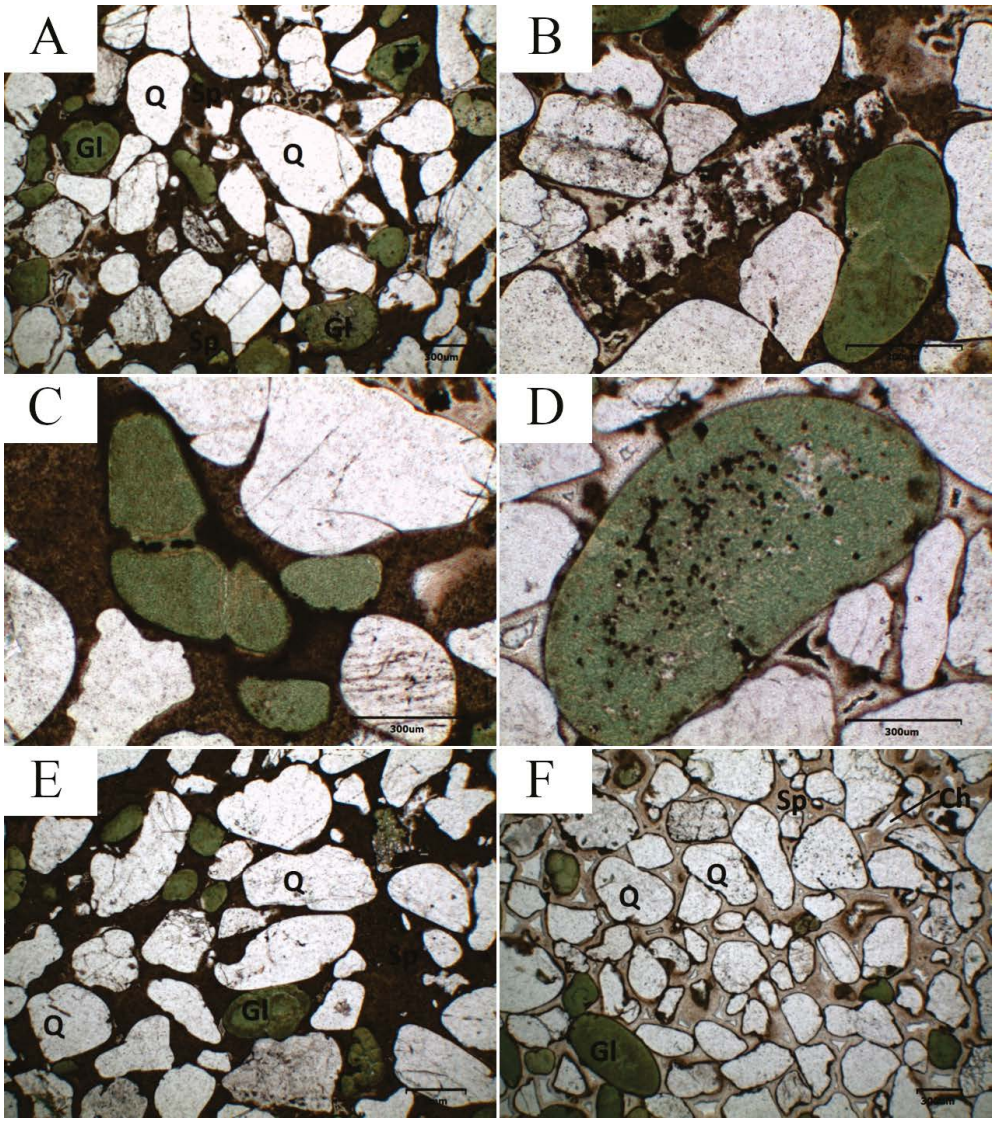


Fig. 6. Photomicrographs taken with the polarizing transmitted light microscope of the quartz-glauconite sandstone from the "Górka Lubartowska-Niedźwiada" deposit
A: Q – quartz, Gl – glauconite, Sp – cement; B: fragment of marine fauna; C: glauconite grain with a smooth surface, without inclusions and traces of etching; D: glauconite grain with dark mineral inclusions (pyrite?); E: matrix cement: Gl – glauconite, Q – quartz, Sp – cement;
F: siliceous regenerative cement: Gl – glauconite, Q – quartz, Sp – cement, Ch – chalcedony

Rys. 6. Obrazy z mikroskopu polaryzacyjnego do światła przechodzącego piaskowca kwarcowo-glaukonitowego ze złoża „Górka Lubartowska-Niedźwiada"
A: Q – kwarc, Gl – glaukonit, Sp – spoiwo; B: fragment fauny morskiej; C: ziarno glaukonitu o gładkiej powierzchni, bez wrostków i śladów nadtrawień; D: ziarno glaukonitu z wrostkami ciemnego minerału (piryt?); E: spoiwo typu matrix: Gl – glaukonit, Q – kwarc, Sp – spoiwo;
F: spoiwo regeneracyjne krzemionkowe: Gl – glaukonit, Q – kwarc, Sp – spoiwo, Ch – chalcedon

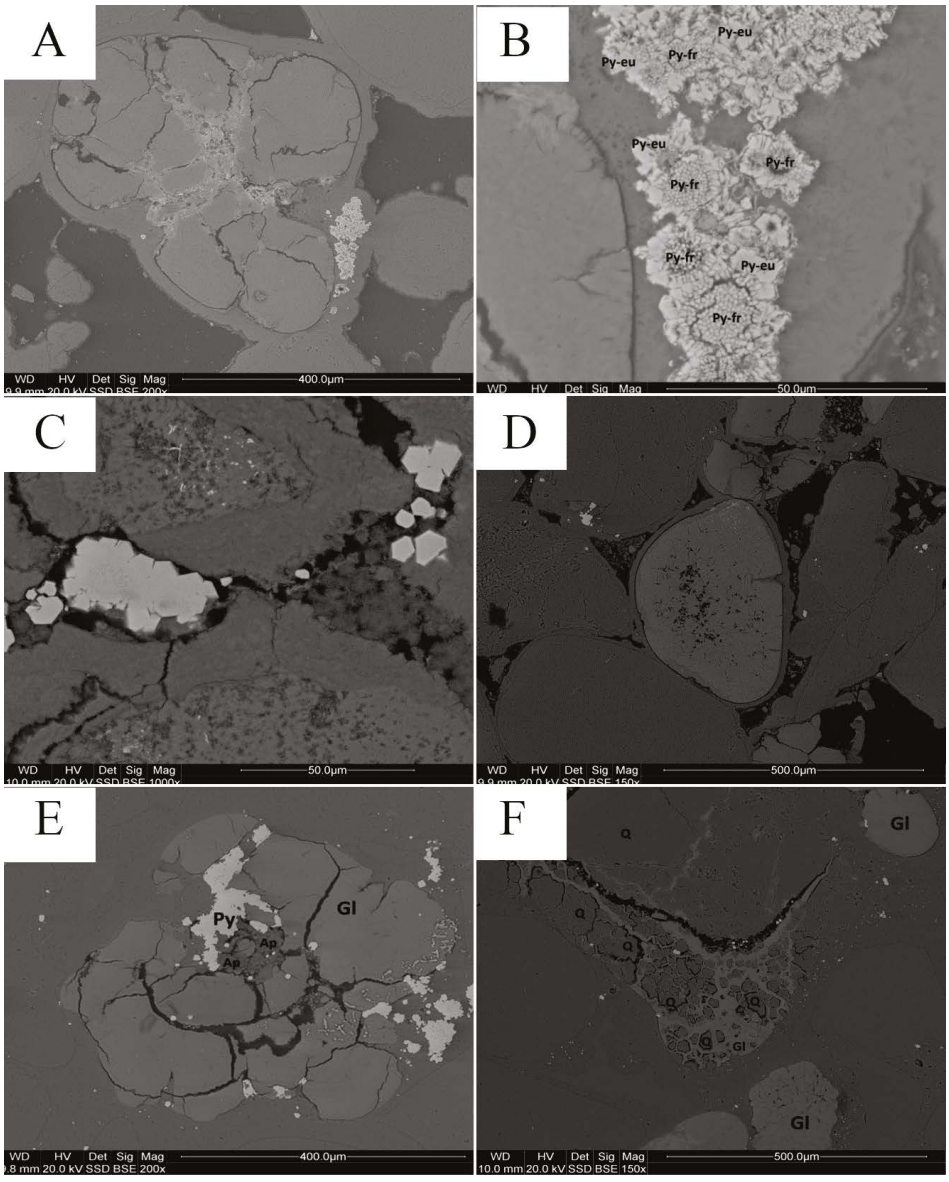


Fig. 7. BSE images of quartz-glauconite sandstone from the "Górka Lubartowska-Niedźwiada" deposit
A – etched and fissured glauconite (Gl) grains with pyrite (Py) inclusions; B – framboidal pyrite (Py-fr) and euhedral pyrite (Py-eu); C – concentration of euhedral pyrite grains (Py) in glauconite; D – glauconite grain (Gl) with a silica rim ($SiO_2$); E – concentrations of calcium phosphate – apatite (Ap) and pyrite (Py) in glauconite (Gl); F – quartz crystals (Q) in the grain of glauconite (Gl)

Rys. 7. Obrazy BSE piaskowca kwarcowo-glaukonitowego ze złoża „Górka Lubartowska-Niedźwiada"
A – nadtrawione i spękane ziarna glaukonitu (Gl) z wrostkami pirytu (Py); B – piryty framboidalne (Py-fr) oraz euhedralne (Py-eu); C – skupienie pirytów euhedralnych (Py) w glaukonicie; D – ziarno glaukonitu (Gl) z obwódką krzemionkową ($SiO_2$); E – skupienia fosforanu wapnia – apatytu (Ap) i pirytu (Py) w glaukonicie (Gl); F – kryształy kwarcu (Q) w ziarnie glaukonitu (Gl)

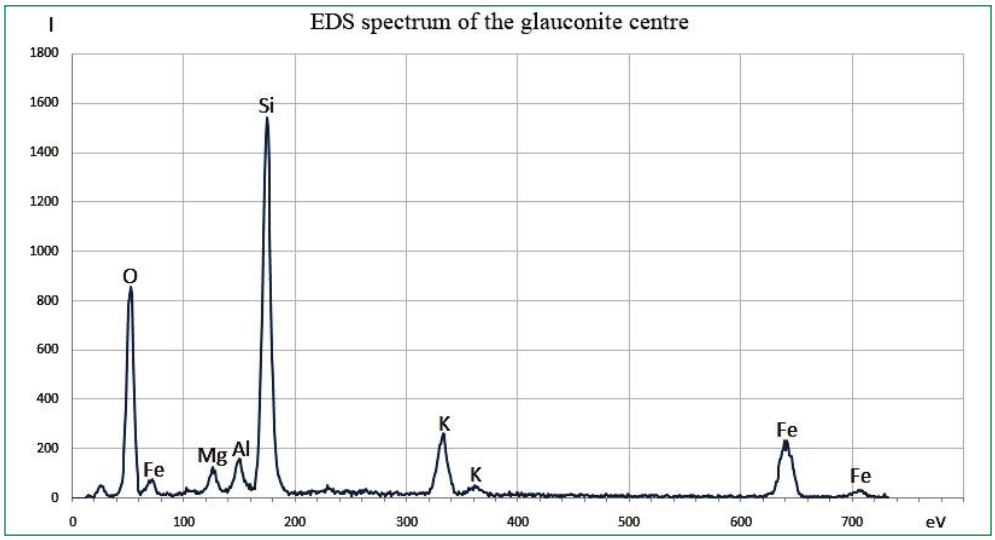


Fig. 8. EDS spectrum of a glauconite grain from the "Górka Lubartowska-Niedźwiada" deposit

Rys. 8. Widmo EDS ziarna glaukonitu z piaskowca ze złoża „Górka Lubartowska-Niedźwiada"

the earlier data from the EDS determinations. Figure 9B shows the spatial distribution of Fe and Ca in the selected glauconite grain. The tendency of Fe to concentrate more on the edges of the glauconite grains can be observed.

The detailed information on the chemical composition of the glauconite was provided by the electron microprobe analyses (Pałasz 2017). The subject of the analyses were grains of the non-homogeneous structure. The greatest differences occur in the concentration of $Al_2O_3$ and FeO, while the share of other components is stable. Glauconite specimens in which the presence of calcium phosphate clusters was determined in their central parts were also examined with the use of the microprobe. Attention is drawn to the fact that the chemical composition of glauconite grains is very diverse, especially as regards $Al_2O_3$, FeO and $K_2O$, whereas the MgO concentration varies within a small range only.

Mineral inclusions in glauconite grains observed in the SEM images were identified using the Raman spectroscopy. The following diagnostic glauconite bands were registered on the RS spectrum: 210, 260, 595 and 694 $cm^{-1}$ (Ospitali et al. 2008), also the bands indicative of the presence of anatase (Fig. 10A, B), i.e. 144, 398, 446, 516 and 639 $cm^{-1}$ were observed (Ohsaka et al. 1978).

### 3.3. Xylite

It is rare to observe such well-preserved fragments of tree branches in the sand, especially since they are millions of years old. The xylite under analysis had an elongated shape with

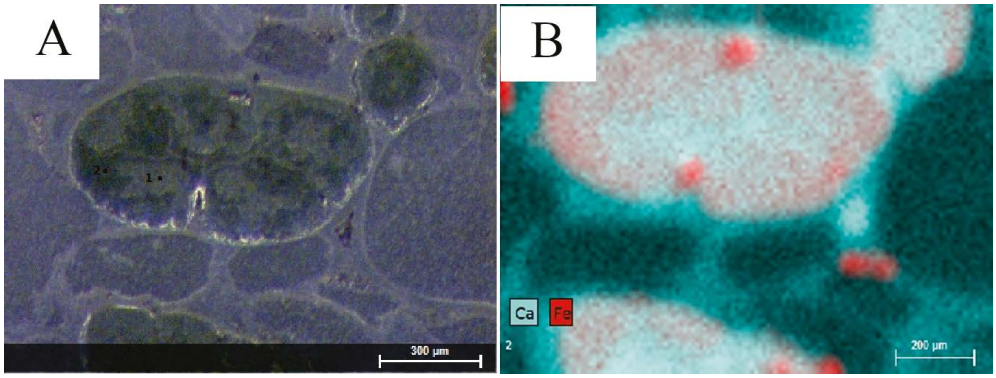


Fig. 9. XRF data. A – glauconite grain of the heterogeneous structure, with marked measurement points; B – distribution map of Fe and Ca content in glauconite grains

Rys. 9. Dane XRF. A – ziarno glaukonitu o niejednorodnej budowie, z zaznaczonymi punktami pomiarowymi; B – mapa rozkładu zawartości Fe i Ca w ziarnach glaukonitu

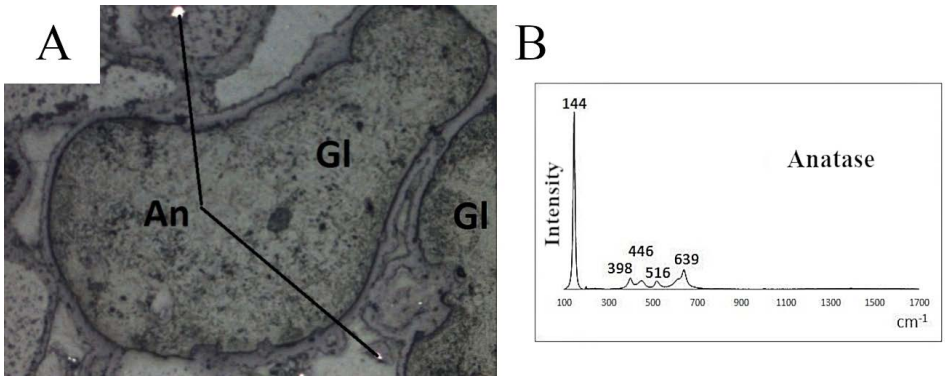


Fig. 10. A – anatase inclusions (An) within glauconite grains (Gl); B – Raman spectrum of anatase

Rys. 10. A – wrostki anatazu (An) w obrębie ziaren glaukonitu (Gl); B – widmo Ramana anatazu

the axial length of 0.1 to 5 cm. Their quantity in the collected sand samples was assessed at 1 vol%. Larger xylites are considerably flattened due to the diagenetic static pressure of the mineral overburden, hence their ellipsoidal shape in the cross-section. The ratio of perpendicular axes in this cross-section is close to 2:1, which is typical of xylites occurring in soft lignite deposits from the area of Poland (e.g. Widera 2013, 2015). The xylites are light-brown and have a dull lustre.

Macroscopically, the xylites do not show any distinct traces of the gelification process (marked by the black color), one exception being the sparse thin bands extending longitudinally to their axes, which are visible on their outer walls. A residual longitudinal splittability

is also preserved (Kwiecińska and Wagner 1997). In the cross-section, the darker, porous outline of the core is also highlighted, while a fibrous fine open knot with partially preserved core is visible on the outer wall.

In the petrographical sense, these are parts of a brittle xylite, gelified moderately in the outer parts (Kwiecińska and Wagner 1997), which is indicative of fragments of twigs or young stems, presumably of coniferous trees.

In the microscopic observations of the xylite cross-section, a large internal part of the axial cylinder can be seen, in which one can distinguish the core and the xylem (wood tissue). Its outer parts are strongly humified and partially gelified. The core was preserved in the form of two elements located next to each other, with ellipsoidal (larger) and sickle-shaped (smaller) forms (Fig. 11A). The central core has a longer axis of up to 2 mm in length, while the smaller is ca. 1 mm long. Both are located eccentrically and surrounded by deformed xylem tissues with an indistinct outline of the annual rings. The cores themselves are composed of a breccia of lignified cell walls whose outer parts (the so-called core crown) are highly gelified, replaced with a porous gel (Fig. 11B). They are strongly porous. The empty pores are frequently arranged longitudinally as the primary fissures formed during the lignification process. In the petrographical sense, they are composed of textoulminite, and the gelified core crown of porigellinite. The twin-core nature of the fossil wood that is rarely observed in xylites is noteworthy. It is a morphological trace left deeper in the branch or stalk after bifurcation, which was observed macroscopically in some of the xylites in the form of a preserved knot.

The core is surrounded by concentrically shaped wood tissues, with a fuzzy outline of the annual rings (Fig. 11C). The so-called late-wood coils are well visible, because they are less damaged, heavily deformed, sometimes flattened or torn apart, visible in the humified mass due to the presence of the anisotropic cellulose. They are empty, in places impregnated with pyrite, but mostly filled with a porous humic gel. Petrographically this is textinite, and submicroscopic fillings of coils and coal background represent porigellinite.

The faint, brown outline of the annual rings in the wood tissues, visible under the transmitted light, are the humified early wood and pith cells. The textinite exhibits distinct anisotropy in the fragments of incompletely humified cellulose and weak fluorescence in light-brown color under blue light, which is only locally stronger in the greenish-yellowish color, typical of the resinite (resin) that partially impregnates the xylites.

The presence of full core radii was not observed, but only of their small fragments in the form of short brown sections, heavily deformed and displaced (Fig. 11D). Such an appearance is not surprising due to the strong humification and gelification of the pith wood tissue. There were also more noticeable traces of the presence of resin bundles, which is confirmed by the well-known morphology of the resin channels and the observed strong resinite fluorescence under the blue light.

The outer part of xylites is a thin coating of humified wood, developed in the form of a fine-grained breccia of cell walls, which is inserted in an almost entirely homogenized humic mass. Petrographically, this is ulminite, with locally preserved bands of textoluminite.

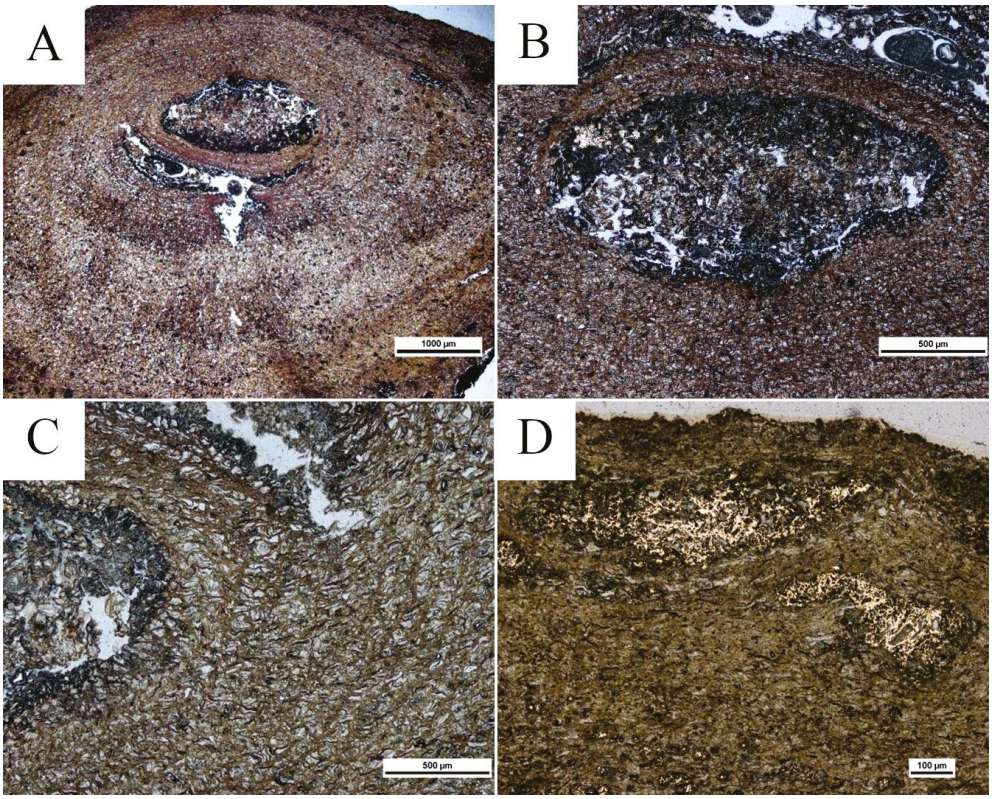


Fig. 11. Photomicrographs of transverse cross-sections of xylites encountered in quartz-glauconite sand from the "Górka Lubartowska-Niedźwiada" deposit
A – double core of xylites and a geometric coaxial arrangement of coils around them; B – axial xylite core structure; C – system of wood coil rings in a xylite; D – highly deformed cells due to compaction and carbonization, partially impregnated with pyrite

Rys. 11. Mikrofotografie przekrojów poprzecznych ksylitów napotkanych w piaskach kwarcowo-glaukonitowych ze złoża „Górka Lubartowska-Niedźwiada"
A – podwójny rdzeń ksylitów i geometryczny współosiowy układ cewek wokół nich; B – struktura osiowego rdzenia ksylitu; C – układ pierścieni cewek drewna w ksylicie; D – silnie zdeformowane komórki wskutek kompakcji i uwęglenia, częściowo impregnowane pirytem

A variety of ulmulite, i.e. euulminite B is visible locally (its presence is indicated by the results of reflectance measurements).

The outermost part of the xylite consists of discontinuous lenses of an organic gel (gelinite) and includes streaks and reticular pyrite impregnation (Fig. 11D). The gelinite is quite homogeneous, in some cases porous. Its lenticular shape is due to the transverse cross-section of xylite (fibrous coating along the xylite axis).

Pyrite occurs in several morphological forms. Most often it is a framboidal pyrite whose individuals have a lenticular shape. The second variety are the reticular forms, created by impregnation or substitution of the wood cell walls with pyrite.

In order to determine the degree of carbonisation, the random reflectance of the euulminite B in the xylite was measured. It is a rather sparse component of xylites, hence the number of measurements was limited to the statistically significant amount (Kwiecińska nad Wagner 2001). The average reflectance of the euulminite B in xylites is 0.25%, with the standard deviation of 0.02% and an empirical range of measurements between 0.21 and 0.28.

## Discussion

The quartz-glauconite sands and the quartz-glauconite sandstone associated with them show a very similar mineralogical composition, which points to the identical source area of the clastic material which these deposits were made from. The vast majority of their grains are characterized by a significant granulometric diversity. The poor degree of sorting of these materials, with the domination of fine grains, as well as the prevalence of well-rounded individuals clearly indicate a long-lasting river transport of these sediments.

The mineralogical composition of both the sand and sandstone (quartz, feldspar, mica and anatase), and in the case of some of the aforementioned phases the distinctive elongated angular shape may imply that the source material could be both acidic igneous rocks of the granite type, and also their volcanic counterparts (a typical habit of the pyrogenic quartz), but also metamorphic rocks. The source could be distant massifs of crystalline rocks undergoing weathering processes as well as volcanic activity products in these areas.

The heavy minerals in the clastic rocks under study are dominated by iron sulphides (pyrite), which are indicative of the euxinic conditions of formation of these rocks, which are characterized by a very low oxygen content or the absence of oxygen in the lower part of the water column, at the simultaneous presence of hydrogen sulphide. The presence of hydrogen sulphide in the solution is related to the decomposing organic matter (Kucha 1981), which creates favourable conditions for the syngenetic growth of glauconite (McRae 1972). The euxinic nature of the formation of the rocks under investigation – especially of the quartz-glauconite sandstone – is also evidenced by the presence of euhedral pyrite accumulations, which grow on framboidal pyrite grains. Similar structures are nowadays found in the euxinic waters of the Black Sea, where syngenetic framboidal pyrite grains form in the water column, and when they reach the critical size of ca. 5 mm they start to sink to the bottom of the basin. After the process of accumulation and burial, they do not grow further, but are enlarged by the growth of euhedral pyrite on them (Wilkin et al. 1996; Zatoń et al. 2008).

The presence of two zones in which a different composition of the cement occurs – a regenerative-silica type and a matrix type is particularly symptomatic of the genetic considerations of the quartz-glauconite investigated sandstone. In each of these zones, one can notice a different manner of grain distribution and density, as well as the size and type of inter-grain contacts. In the zone where the silica type cement dominates, the grains are much

more densely packed and smaller, and the intergranular contacts are as a rule linear or even point-shaped. There is a regenerative rim of silica on each of the grains, and fine-crystalline chalcedony occurs in the open spaces. The occurrence of this type of cement is typical of the advancing process of diagenesis, and at the same time the formation of the aforementioned regenerative rims and chalcedony crystallization are related to the progress of glauconitization. This involves, e.g. the release of silica from the glauconite grains, while aluminum is introduced in the place in the tetrahedral layer. This implies that the sediment was in an area where locally more advanced diagenetic processes were taking place.

Glauconite grains, present in both the quartz-glauconite sands and their diagenetically altered counterparts, are characterized by a variety of morphological forms and the presence of numerous inclusions of various form. The most abundant are the inclusions of pyrite crystals, most frequently filling fissures within glauconite grains. This could be indicative of their crystallization from the migrating solutions within unconsolidated sediments. The process of glauconite pyritization observed to the same extent in grains from the sand and sandstone, demonstrates that reduction conditions prevailed during sedimentation and diagenesis of the sediments, thus the environment of their formation was quite stable. Ivanovskaya et al. (2010) pointed out that pyritization of glauconite was more intensive in the case of larger individuals (> 0.4 mm), which was also confirmed by the analyses performed (see Fig. 4C).

The SEM-EDS and RS investigations and the results of chemical analyses with the use of the electron microprobe also confirmed the presence of calcium phosphate (apatite?) in some of the glauconite grains. The formation of autigenic phosphates takes place in an anaerobic or very low oxygen environment and at increasing water temperature (Kuhn and Pizon 1987; Carson and Crowley 1993). In turn, Coleman (1985) believes that the association of glauconite with phosphates is formed under conditions of decreasing pH (the effect of organic matter decomposition) and at a rather slow rate of diagenesis. This is, therefore, a proof of the locally varying nature of the environment in which the glauconite rocks under analysis were formed (a transition zone between the anaerobic and aerobic zones). Undoubtedly, it is also worth noting that anatase inclusions were found within the glauconite grains (RS). Their occurrence may be related to the original rock material transported by a river from remote areas to the sedimentation basin, but it may also be related to the decomposing organic matter, which gave rise to the formation of a syngenetic glauconite.

A distinctive feature of the glauconite grains under study is the variety of the chemical composition within individual specimens of this mineral. This is indicated by, for example, observations in the field of the transmitted light microscope as well as by SEM images. The structural heterogenesity is emphasized by the variable saturation of the green color, from light to dark green. The XRF studies have shown that these zones also differ in their chemical composition. In the dark-green areas the share of Fe, K, Mg and Al is clearly increasing, i.e. the share of all of the characteristic chemical elements, in relation to which the degree of maturity of the glauconite is determined. As far as iron is concerned, its largest accumulations occur in marginal zones of the glauconite individuals.

The change of the chemical composition and shades of glauconite colors was directly influenced by the glauconitization process. It led to the exchange of ions in the tetrahedral layers (Al for Si) and octahedral layers (Fe and Mg for Al) and resulted in the increase in the potassium content in the interlayer spaces. These changes were well documented by the results of the electron microprobe analysis. The hypothesis was confirmed that dark green areas of glauconite grains are more genetically evolved. The determined potassium content (ca. 6 wt%) in the glauconite grains implies that according to the classification proposed by G.S. Odin and A. Matter (1981) and A. Amorosi et al. (2007) the glauconite can be classified as mature (6–8% $K_2O$ by weight) and even highly mature glauconite (> 8% $K_2O$ by weight) which is a potential raw material, e.g. for the production of mineral fertilizers.

In the case of quartz-glauconite sand, valuable genetic information is provided by the fragments of carbonized wood found in the roof part and sporadically throughout the entire glauconite layer (see Fig. 1). Only the central part of the axial cylinder, consisting of a double core and an inner part of the wood (heartwood), the stem or branch of the most probably coniferous wood was preserved in the xylite studied. The presence of a twin core, rare in xylites, implies the start of the branch deeper in the wood.

The said xylite fragments belong to the brittle variety and are slightly weathered. They show quite deep-reaching tissue destruction, that resulted from coalification under conditions of weaker insulation from the mineral overburden, hence the humification process is advanced; there are no external parts of the phloem and periderm (cork and phellogen) in the branches. Also, heartwood shows a considerable degree of destruction. The wood adhering to the cores and especially tracheids (coils) of late (summer) wood was best preserved. The deformed outline of annual rings may be indicative of a moderately warm climate with short seasons of cooling (the end of the Paleogene).

The random reflectance of euulminite B obtained in the measurements points to a low degree of coalification of the xylites analysed (ortho lignite). This is a typical value for the soft lignite from the Tertiary Coal Hemisphere around the Atlantic (Sýkorova et al. 2005). With reference to the coal deposits in the Polish Lowlands, this applies to the so-called epeirogenic deposits (or stratified deposits), with a lenticular form, differing from the tectonic trough deposits, where the random reflectance is much higher. It is indicative of the conditions of coalification under a small overburden. The small, corrected asymmetry coefficient (0.034) and the kurtosis value – 0.933 typical of the normal (Gausian) distribution, point to a single-stage, continuous coalification period and almost imperceptible changes in the type of weathering.

## Conclusions

1. Glauconite grains from “Górka Lubartowska-Niedźwiada” deposit presents diversity of structural properties in the term of morpholohy and the presence of impurities. The chemical composition of glauconite also varies within the host-rock as well as within

the single grain. This suggests different environmental conditions of their formation and alteration.

2. The potassium content in glauconite (average above 6 wt% $K_2O$) should be increased in the process of technological enrichment to strengthen its potential as a raw material for the production of mineral fertilizers.
3. The glauconite conglomerate obtained from the sands of the "Górka Lubartowska--Niedźwiada" deposit exhibits the significant amount of iron (average ca. 20 wt% $Fe_{tot}$), mainly incorporated into pyrite and marcasite crystal lattices. The contamination of those minerals is difficult to remove due to technological limitations; however their presence does not depreciate this material for industrial purposes.
4. Further studies should be performed on quartz specimens which occur within sands in significant amount (ca. 45 vol%).

*Reviewers are acknowleged for their frendly remarks. This work was financially supported by the AGH University of Science and Technology (Krakow, Poland), research projects No. 11.11.140.158, and 11.11.140.161.*

## REFERENCES

Amorosi et al. 2007 – Amorosi, A., Sammartino, I. and Tateo, F. 2007. Evolution patterns of glaucony maturity: A mineralogical and geochemical approach. *Deep Sea Research Part II: Topical Studies In Oceanography* 54(11–13), pp. 1364–1374.

Baldermann et al. 2012 – Baldermann, A., Grathoff, G. and Baldermann, C. 2012. Micromilieu-controlled glauconitization in fecal pellets at Oker (central Gemrany). *Clay Minerals* 47(4), pp. 513–538.

Bodelle et al. 1969 – Bodelle, J., Lay, C. and Parfenoff, A. 1969. Age des glauconiescretacees du sud-est de la France (2:Vallee de l'EsteronAlpes-Maritimes). Resultats preliminaires de la methode potassium-argon. *Comptes Rendus de l'Académie de Sciences* 268D, pp. 1576–1579 (*in French*).

Bogdasarow et a.l 2016 – Bogdasarow, M.A., Natkaniec-Nowak, L., Криницкая, M.B., Kutyła-Olesiuk, A., Drzewicz, P. and Czapla, D. 2016. The prospects of development of geological-genetic model of amber-bearing deposits of Poland, Belarus and Ukraine. The reports of the Joint Scientific Conference titled "Problems of the rational use of natural resources and sustainable development of Polesie", Minsk, Belarus, 14–17.09. 2016; 450–454 (*in Russian*).

Burst, J. 1958. Glauconite pellets – their mineral nature and applications to stratigraphic interpretations. *Bulletin of the American Association of Petroleum Geologists* 42, pp. 310–327.

Carson, G.A. and Crowley, S.F. 1993. The glauconite–phosphate association in hardgrounds: examples from the Cenomanian of Devon, southwest England. *Cretaceous Research* 14, pp. 69–89.

Coleman, M.L. 1985. Geochemistry of diagenetic non-silicate minerals: kinetic considerations. *Philosophical Transactions of the Royal Society of London* A315, pp. 39–56.

Evernden et al. 1961 – Evernden, J.F., Curtis, G.H., Obradovich, J. and Kistler, R. 1961. On the evaluation of glauconiteandillite for dating sedimentary rocks by the potassium-argon method. *Geochimica and Cosmochimica Acta* 23, pp. 78–99.

Foster, M.D. 1951. Geochemical Studies of Clay Minerals. The Importance of exchangeable magnesium and cation exchange capacity in the study of montmorillonite clays. *American Mineralogist* 36, pp. 717–730.

Foster, M.D. 1969. Studies of celadonite and glauconite. *Professional Paper United States Geological Survey* 614-F, 17 pp.

Franus, M. 2010. *Zastosowanie glaukonitu do usuwania śladowych ilości metali ciężkich.* Lublin: Politechnika Lubelska, pp. 31–39.

Grim, R.E. 1953. *Clay mineralogy.* New York: McGraw-Hill Book Company, Inc. 384 pp.

Hower, J. 1961. Some factors concerning the nature and origin of glauconite. *American Mineralogist* 46(1961), pp. 313–334.

Ivanovskaya et al. 2010 – Ivanovskaya, T.A., Tsipurskiy, S.I., Cherkashin, V.I. and Yakhontova, L.K. 2010. Postsedimentation alteration of glauconite in southeast Yakutia riphean beds. *International Geology Review* 27(12), pp. 1451–1460.

Kazakov, G.A. 1964. The use of glauconite to determine the absolute age of sedimentary rocks [In:] *Khimia Zemnoi Kory, Akademia Nauk. S.S.S.R., Trudy Geokhimicheskoi Konferencji* 2, pp. 539–551.

Kłapyta, Z. 2008. *Właściwości powierzchniowe sorbentów mineralnych.* Kraków: Uczelniane Wydawnictwo Naukowo-Dydaktyczne AGH, pp.77–86.

Krzowski, Z. 1995. *Glaukonit z osadów trzeciorzędowych regionu lubelskiego i możliwości jego wykorzystania do analiz geochronologicznych.* Lublin: Wydaw. Uczelniane Politech. Lubelskiej, 130 pp.

Kucha, H. 1981. Precious metal alloys and organic matter in the Zechstein copper deposits, Poland. *Tschermaks Mineralogische und Petrographische Mitteilungen* 28, pp. 1–16.

Kuhn, A. and Pizon, A. 1987. Warunki sedymentacji serii fosforytonośnych górnego albu i cenomanu rejonu Gościeradów – Salomin (NE Obrzeżenie Gór Świętokrzyskich). *Przegląd Geologiczny* 35(4), 169–175.

Kwiecińska, B. and Wagner, M., 1997. *Classification of qualitative features of brown coal from Polish deposits according to petrographical chemical and technological criteria*. Kraków: PPGSiEM, 87 pp.

Kwiecińska, B. and Wagner, M., 2001. *Możliwość zastosowania refleksyjności jako metody badawczej w klasyfikowaniu i technologicznej ocenie jakości węgla brunatnego.* Kraków: Wyd. AGH, 35 pp.

Łozińska-Stępień et al. 1986 – Łozińska-Stępień, H., Rytel, A. and Saliński, P. 1986. Szczegółowe *objaśnienia do mapy geologicznej Polski*, *Arkusz Leszkowice*. Warszawa: Wydawnictwo Geologiczne.

McRae, S.G. 1972. Glauconite. *Earth-Science Reviews* 8, pp. 397–440.

Moore, D. and Reynolds, R. 1997. *X-ray Diffraction and the identification and Analysis of Clay Minerals*. 2nd ed. Oxford University Press, 378 pp.

Odin, G.S. and Matter, A. 1981. De glauconiarum origine. *Sedimentology* 28, pp. 611–641.

Odin, G.S. and Fullagar, P.D. 1988. Geological significance of the glucony facies [In:] Odin, G.S. red. *Green Marine Clays: Developments in Sedimentology.* Elsevier, pp. 295–332.

Ospitali et al. 2008 – Ospitali, F., Bersani, D., Di Lonardo, G. and Lottici, P. 2008. 'Green earths': vibrational and elemental characterization of glauconites, celadonites and historical pigments. *Journal of Raman Spectroscopy* 39, pp. 1066–1073.

Ohsaka et al. 1978 – Ohsaka, T., Izumi, F. and Fujiki, Y. 1978. Raman Spectrum of Anatase. *Journal of Raman Spectroscopy* 7(6) pp. 321–324.

Pałasz, K. 2017. *Charakterystyka mineralogiczna glaukonitu z okolic Niedźwiady (woj. lubelskie)*. Kraków: Archiwum KMPiG WGGiOŚ AGH, 42 pp.

Pettijohn et al. 1972 – Pettijohn, F.J., Potter, P.E., and Siever, R. 1972. *Sand and sandstone.* New York: Springer-Verlag, 618 pp.

Schieber, J. 2002. Sedimentary pyrite: A window into the microbial past. *Geology* 30(6), pp. 531–534.

Shively, R. and Weyl, W. 1951. The Color Change of Ferrous Hydroxide upon Oxidation. *The Journal of Physical and Colloid Chemistry* 55, pp. 512–515.

Smaill, J. 2015. *Geochemical Variations in Glauconitic Minerals: Applications as a Potassium Fertiliser Resource*. MSc thesis. New Zealand: University of Canterbury, pp. 4–7.

Soni, M. 1990. On the possibility of using glauconite sandstone as a source of raw material for potash fertilizer. *Indian Mining and Engineering Journal*, pp. 3–10.

Smulikowski, K. 1953. Rozważania na temat glaukonitu. *Przegląd Geologiczny* 1(2), pp. 8–12.

Sýkorova et al. 2005 – Sýkorova, W.P., Christanis, K., Wolf, M. and Florest, D. 2005. Classification of huminite – ICCP System 1994. *International Journal of Coal Geology* 62(1), pp. 85–106.

Triplehorn, D.M. 1966. Glauconite provides good oil search data. *Worm Oil* 162, pp. 94–97.

Tyler, S.A. and Bailey, S.W. 1961. Secondary glauconite in the Biwabic iron-formation of Minnesota. *Economic Geology* 56, pp. 1033–1044.

Valanchene et al. 2006 – Valanchene, V., Mandeikite, N. and Urusowa, E. 2006. Intensity of coloring in ceramics with glauconite additives. *Glass and Ceramics* 3, pp. 23–25.

Warshaw, C.M. 1957. *The Mineralogy of Glauconite*. Thesis, Pennsylvania State University, University Park, PA, 155 pp.

Wilkin et al. 1996 – Wilkin, R., Barnes, H. and Brantley, S. 1996. The size distribution of framboidal pyrite in modern sediments: an indicator of redox conditions. *Geochimica and Cosmochimica Acta* 60, pp. 3897–3912.

Widera, M. 2013. Remarks on determining of the compaction coefficient of xylites for the first Middle-Polish lignite seam in central Poland. *Przegląd Geologiczny* 61, pp. 304–310.

Widera, M. 2015. Compaction of lignite: a review of methods and results. *Acta Geologica Polonica* 65, pp. 367–368.

Gong et al. – Gong, Y. M., Shi, G.R., Weldon, E.A. and Yuan-Sheng Du. 2008. Pyrite framboids interpreted as microbial colonies within the Permian Zoophycos spreiten from southeastern Australia. *Geological Magazine* 145(1), pp. 95–103.

Zatoń et al. 2008 – Zatoń, M., Rakociński, M. and Marynowski, L. 2008. Pyrite framboids as paleoenvironmental indicators (*Framboidy pirytowe jako wskaźniki paleośrodowiska*). *Przegląd Geologiczny* 56(2), pp. 158–164 (*in Polish*).

## "GÓRKA LUBARTOWSKA-NIEDŹWIADA" DEPOSIT (E POLAND) AS A POTENTIAL SOURCE OF GLAUCONITE RAW MATERIAL

Keywords

"Górka Lubartowska-Niedźwiada" deposit, quartz-glauconite sands, glauconite, xylite

Abstract

The main subject of research in this paper is glauconite with its useful parameters, which is the object of exploitation in the "Górka Lubartowska-Niedźwiada" deposit. The main glauconitic horizon (lower Eocene) is built by loamy fine-grained and medium greenish sands with marine fauna and fragments of amber (ca. 7 m thick). Thin lamins and pockets of silts containing phosphorites and also glauconitic sands with underlaying very thin quartz-glauconitic sands are found at the bottom of this layer. The glauconite deposit in "Górka Lubartowska-Niedźwiada" is an amount of ca. 30% by volume of the main glauconitic horizon. Glauconite of the 1M polytype (XRD) shows large granulometric and morphological differentiation (SEM-EDS). It frequently contains aggregations of euhedral or framboidal pyrite grains (RS), which is indicative of the euxinic nature of the formation environment of the rocks under study. The individual glauconite grains show distinct chemical variability, manifested in a lower share of $Al_2O_3$ and an increased content of MgO and CaO (EPMA, XRF). At the same time, a large share of $K_2O$ (above 8% by weight) allows it to be included in highly matured glauconite, thus it can be considered as a potential raw material for the production of mineral fertilizers. The association of glauconite with phosphates (SEM-EDS) and anatase inclusions in the grains of glauconite (RS) indirectly point to the contribution of the decomposing organic matter to the formation of grains of this mineral. The xylite fragments preserved in the sediment show a low degree of coalification, which is typical of soft lignite. This also shows that the transformation process was taking place under a relatively small overburden.

**ZŁOŻE „GÓRKA LUBARTOWSKA-NIEDŹWIADA" (E POLSKA) JAKO POTENCJALNE ŹRÓDŁO SUROWCA GLAUKONITOWEGO**

Słowa kluczowe

złoże „Górka Lubartowska-Niedźwiada", piaski kwarcowo-glaukonitowe, glaukonit, ksylit

Streszczenie

Złoże piasków glaukonitowych „Górka Lubartowska-Niedźwiada" znajduje się na obszarze Niziny Podlaskiej (E Polska). Właściwy horyzont glaukonitowy (dolny eocen) budują silnie zailone, drobno- i średnioziarniste piaski, barwy zielonkawej, zawierające faunę morską a także okruchy bursztynu (ok. 7 m miąższości). W spągu tych osadów pojawiają się drobne laminy i soczewki zailonego, zdiagenezowanego mułku glaukonitowego z otoczakami i konkrecjami fosforytów oraz warstwa drobno- i średnioziarnistych piasków glaukonitowych, podścielona bardzo drobną laminą zwartego piaskowca kwarcowo-glaukonitowego. Badaniom poddano piaski kwarcowo-glaukonitowe, próbki piaskowca kwarcowo-glaukonitowego oraz 10 drobnych kawałków ksylitu z osadów czwartorzędowych dolnych. Glaukonit obecny w tych osadach w politypie 1M wykazuje duże zróżnicowanie granulometryczne i morfologiczne. Tworzy formy agregatowe, zazwyczaj zawierające framboidalne lub euhedralne kryształy pirytu wskazujące na euksyniczny charakter środowiska powstawania badanych skał. Glaukonit ten zawiera wyraźnie niższy udział glinu ($Al_2O_3$), natomiast podwyższony udział magnezu (MgO) i wapnia (CaO). W analizowanych ziarnach glaukonitu średni udział $K_2O$ jest wysoki, zatem można go zaliczyć do glaukonitu wysoko dojrzałego. Mimo stosunkowo wysokiej zawartości żelaza może być on potencjalnym surowcem do produkcji nawozów mineralnych. Asocjacja glaukonitu z fosforanami (SEM-EDS) oraz wrostki anatazu w ziarnach glaukonitu (RS) pośrednio wskazują na udział rozkładającej się materii organicznej w tworzeniu się ziaren tego minerału. Zachowane w osadzie fragmenty ksylitów wykazują niski stopień uwęglenia, co jest typowe dla miękkiego węgla brunatnego. Świadczy to jednocześnie, że proces przeobrażeń zachodził pod stosunkowo niedużym nadkładem.